# CHAPTER 3
# MODELING AND PERFORMANCE EVALUATION PROCEDURES FOR STEEL MOMENT FRAME STRUCTURES

**Abstract**: Modeling issues pertinent to steel special moment-resisting frame (SMRF) structures under seismic loads are discussed first in this chapter, followed by description and modeling of an example perimeter steel SRMF that will be used throughout this study. Different analysis procedures are briefly outlined for evaluating seismic structural performance, with emphasis on the static pushover analysis. Information of seismic inputs for this study is provided at the end.

## 3.1 Modeling of steel moment frames for seismic loads

### 3.1.1 Overview

The equivalent lateral force procedure in 2000 NEHRP seismic provisions permits an elastic analysis for seismic design of steel moment resisting frame structures that are represented by simple linear elastic models with centerline dimensions. A building system designed according to these code provisions typically has lower seismic resistance than what can keep the structure elastic under design earthquakes. Inelastic structural responses are therefore expected when subject to design earthquakes and are accounted for approximately through amplification factors provided in these provisions.

Design optimization of seismic steel frame structures to be investigated in subsequent chapters requires accurate evaluation of actual seismic demands on code-compliant alternative designs. A bare-frame linear elastic model with centerline dimensions, which proved to be good for design purposes, is inadequate for estimating seismic demands when inelastic responses are significant (Gupta and Krawinkler 1999). Nonlinear structural models are thus required in which

contributing structural elements that comprise the entire structural system, including moment frames (beams, columns, panel zones, beam-to-column connections) and interior gravity frames (gravity column and beams, shear connections) as well as non-structural components (cladding, partitioning walls), may all need to be modeled appropriately.

Use of clear member dimensions as opposed to simple centerline dimensions improves the accuracy in performance evaluation. Steel structures dissipate most of seismic energy through material hysteresis when subject to cyclic seismic loading, which necessitates modeling of nonlinear steel member behaviors in a realistic manner. Geometrical nonliearities are also significant when large gravity loads act on deformed structural configuration. Effects of panel zone and beam-to-column connection rigidities on seismic structural behavior as observed in laboratory tests should also be addressed properly. Moreover, possible degradation/loss in strength and/or stiffness of connections due to fractures needs to be modeled in detail. The following sub-sections summarize techniques that are most relevant to modeling of steel frames buildings under seismic loads.

### 3.1.2 Nonlinear steel members

Assuming constant cross-sectional properties over the entire element length, a steel beam member in a moment frame is usually modeled in structural analysis software such as DRAIN-2DX (Prakash et al. 1993) by an elastic element with point plastic hinges at both ends. A nonlinear rotational spring element is used to simulate the behavior of plastic hinges, with a bilinear moment-rotation relationship defined by yield strength and a constant post-yield strain-hardening ratio (typically 3% for steel members).

For post-Northridge steel frame designs, the plasticity zone in the beam is forced away from the column face using either cover plated designs or reduced beam sections (FEMA-267 1995).

Accordingly, point plastic hinges in modeling of beam elements should be located at a prescribed distance away from the column face with proper strength and/or stiffness modification (Gupta and Krawinkler 1999).

For columns where higher axial forces are typically present, plasticity may spread over a relatively larger region; as a result, point plastic hinge idealization is not justifiable (Gupta and Krawinkler 1999). On the other hand, formation of plastic regions in columns are very much discouraged or even not allowed in the real-world practice. For example, the AISC seismic provisions (AISC 1997, 2000) require a strong-column-weak-beam mechanism in seismic steel design. Under this criterion, possible plasticity regions are mostly confined to take place in beams; columns are strong enough and essentially remain elastic. Column yielding is allowed only at the building base or roof level. Thus, global collapses are hopefully avoided and post-earthquake rehabilitation work is greatly eased. Therefore, use of the same modeling technique (i.e., point plastic hinges plus elastic elements) for column members may not cause significant accuracy problems under the present design practice (Gupta and Krawinkler 1999).

### 3.1.3 Panel zones

Modern seismic design codes permit use of excellent panel zone hysteresis to dissipate part of seismic energy under design earthquakes. Code guidelines usually provide design shear strength requirements for panel zones. Very weak panel zones with excessive shear deformation at a design force level, which may have detrimental effects on welded connections (Gupta and Krawinkler 1999), should nevertheless be avoided. Strength and stiffness of panel zones should be incorporated in the analytical model for better seismic response prediction of the structural system.

The simplest panel zone representation is an elastic "scissors" model, where beams and column elements, tied by a rotational spring, frame into the panel zone region by rigid links with a beam hinge at the panel zone center; the resulting structural model is usually stiffer than the centerline model, as the stiffening effects of rigid links overwhelm the softening effects of the spring element (Foutch and Yun 2002). As a more advanced nonlinear panel zone model, rigid beam-column elements are used as boundary elements to construct a parallelogram of full panel zone dimensions; the shear strength and stiffness of the panel zone is modeled by providing a tri-linear rotational spring for any one corner of the panel zone together with pin connections for the other three corners (Foutch and Yun 2002).

### 3.1.4 Beam-to-column connections

Both shear and moment beam-to-column connections exist in steel frame buildings. Shear connections are mainly used for interior gravity frames. Moment connections in perimeter moment resisting frames are of two types: fully restrained (i.e., rigid) and partially restrained (i.e., semi-rigid). Rigid connections represent an idealized situation where infinite connection stiffness is assumed and bending moments applied on these connections can be fully transferred to the neighboring members. A more realistic treatment is to explicitly consider connection flexibility, which leads to semi-rigid connection models. The most widely used analytical moment-rotational relationship for semi-rigid connections is a four-parameter power model (Richard and Abbott 1975; Hsieh and Deierlein 1990), which originally represents only the monotonically increasing loading history. To account for the hysteresis behavior of semi-rigid connections under cyclic seismic loading, the four-parameter power model is extended to represent both unloading and reloading behaviors in moment-rotation curves (Colson 1991; Huh and Haldar 2002).

Strength and/or stiffness degradation in hysteresis loops were observed in laboratory tests, which also need to be modeled for better simulation of actual seismic behaviors. By calibrating observed patterns from available experimental data of representative connection types, Foutch and Yun (2002) were able to construct in DRAIN-2DX empirical analysis models for hysteresis loops with strength/stiffness degradation due to fracture, via a Foutch-Shi element (Foutch and Shi 1997). Wang and Wen (2000) developed a smooth analytical hysteresis model using a modified Bouc-Wen model to account for asymmetry in hysteresis loops and a slip-lock element to address the slip and pinching phenomena in fractured connections. Luco and Cornell (2000) also studied effects of brittle connection fractures on seismic drift demands of steel moment frames.

### 3.1.5 P-delta effects due to interior gravity loads

For seismic steel building designs with perimeter moment resisting frame systems, interior frames are typically designed to carry only gravity loads and they will deform along with the perimeter moment frames when subject to lateral loads. P-delta effects due to interior gravity loads that are transferred to the moment frames via floor slab interactions can be significant when a frame undergoes large lateral displacements and have to be addressed properly.

Following Foutch and Yun (2002), a fictitious column element with very high axial stiffness and negligible flexural stiffness is connected to the moment frame model using rigid links with pin connections at both ends. Gravity loads tributary to the relevant interior frames are then applied to this dummy column at each floor level. Therefore, this dummy column can deflect together with the original moment frame without any additional bending moment resistance.

To further consider lateral resistance provided by interior gravity frames (columns, beam, and shear connections that could produce bending moment resistance due to composite action

between floor slabs and steel girders) and moment frames (weak-axis columns) in the orthogonal direction, a fictitious gravity one-bay frame may be added to the original moment frame model (Foutch and Yun 2002). Beams, columns, and rotational springs of this dummy frame bay have equivalent stiffness and strength properties of those of the interior gravity frames and of the orthogonal moment frames, respectively. Detailed relevant conversion procedures can be found in Gupta and Krawinkler (1999).

### 3.1.6 Other modeling issues

In addition to the above modeling concerns, there exist other issues that need to be considered appropriately if possible. For example, torsional interaction of structural components due to spatial seismic excitations and/or structural irregularity may alter significantly performance estimates resulting from a simple 2D frame model; non-structural components (cladding, partitioning walls, etc.) also contribute extra stiffness to the structural system.

No matter how refined a structural model is, there exist many uncertainties in depicting behavioral characteristics of structural components as well as the entire structural system. As a result, assumptions have to be made, for example, regarding strength, stiffness, and deformation levels of different structural components. Sensitivities of both element and system level demands to these different modeling assumptions were systematically studied in Gupta and Krawinkler (1999). In addition, factors that contribute to structural responses may not sometimes be very well modeled due to lack of support from field observations and/or experimental data. The increased modeling complexity, however, seem unjustifiable due to uncertainties inherent in the estimation of both demands and capacity. In view of these, structural models with moderate sophistication may be desirable that can still capture major characteristics of seismic structural responses.

## 3.2 Frame modeling for the present study

### 3.2.1 An example steel moment frame

As shown in Figure 3.1, the example structure used in this study is a regular plane five-story four-bay steel special moment-resisting frame (SMRF) which constitutes one of the two identical north-south perimeter frames in a 100 ft (30.48 m) by 150 ft (45.72 m) office building fixed at the base, with a height of 67 ft (20.42 m) assumed to be built in Los Angeles area, California. Symmetric pairs of members about the vertical centerline of this SMRF are of the identical section types, respectively; in addition, all beam members across the same floor (or roof) are grouped with a single section type (Figure 3.2).

In a realistic steel frame design practice, locations of column splice are usually determined before member sizing is performed due to shippability/erectability concern of long column shafts. Columns spanning two to four floors are generally recommended to simplify its construction. To simulate this practice, column splices are assumed to be located at a distance above the second floor level for construction consideration. In order to simplify the analysis, it is assumed that column sizes change exactly at the second floor level. There are therefore eleven design variables in total: six for column members and five for beam members (Figure 3.2). The labor cost needed for a column splice is assumed equivalent to 500 lbs (2.2 KN) of Grade 50 steel (Carter et al. 2000).

Following Kang and Wen (2000), dead load intensities for the floor and roof levels are 76 psf (3.64 KPa) and 67 psf (3.21 KPa), respectively; live load intensities for the floor and roof levels are 45 psf (2.15 KPa) and 16 psf (0.77 KPa), respectively; exterior wall and façade intensities are 30 psf (1.44 KPa) for all stories. The SMRF is expected to resist half of the lateral seismic force of the entire building.

The nominal steel strength is usually used for design purposes. To attain realistic seismic structural responses, the expected steel strength should be applied instead. In this study, A36 and A-572 steel materials, which are assumed for beam and column members respectively, have nominal yield values of 36 ksi (248.2 MPa) and 50 ksi (344.7 MPa), respectively, while their expected yield values are 49.2 ksi (339.2 MPa) and 57.6 ksi (397.1 MPa), respectively, based on the SSPC documents (1994).

### 3.2.2 Modeling considerations

The main goal of the present study is to develop general seismic design optimization procedures for steel SMRF structures considering multiple merit objective functions, some of which are based on evaluation of actual seismic performance of code-conforming alternative designs. A simplified analytical steel frame model may be justifiable that accounts for major contributions of structural elements to seismic responses, in particular, to displacement-related responses.

The following modeling issues are considered in the present study:

- A bare-frame model of the plane steel SMRF structure is created in the DRAIN-2DX, where centerline beam-column elements (Type 2) without strength/stiffness deterioration are used to model all beams and columns with a 3% strain hardening ratio for point plastic hinges located at the element ends. Torsional effects are not considered.
- Full restraints are assumed in the minor axis directions of column members and only buckling strengths of columns in the major axes are considered. Compact sections are used and adequate lateral bracing is applied where appropriate, which avoid, at an assurance level provided by the design provisions, the occurrence of strength and

stiffness deterioration due to local and lateral torsional buckling in severe earthquakes. Practical design details such as cover plates and the reduced beam sections are not included.

- P-delta effects are modeled using the equivalent gravity column technique as described in Section 3.1.5. Stiffness due to interior gravity frames, which renders larger drift capacities and smaller drift demands (Foutch and Yun 2002), is not considered.
- Rigid connections are assumed, that is, neither ductile nor brittle connection behaviors will be modeled. It is known that pre-qualified moment connections for post-Northridge designs will unlikely experience significant fracture problems.
- Panel zone deformation (shear distortion) is neglected, which will partly counteract the effects of centerline dimensions assumption on quantification of lateral structural deformation. It is noted that panel zone designed in accordance with the current code provisions may be weak enough to attract most of the inelastic deformations under designated earthquakes, which will cause undesirable weld fractures in the connections (Gupta and Krawinkler 1999). Stiffer panel zones may therefore be needed in a practical design.

## 3.3 Seismic performance evaluation procedures

### 3.3.1 Overview

In order to evaluate seismic performance of steel SMRF designs, structural analyses are conducted to predict relevant response parameters using appropriate analytical structural models that represent strength and deformation characteristics of building systems, as discussed in

Section 3.2. Four alternative evaluation procedures in FEMA-273 (1997) and FEMA-350 (2000) are briefly described as follows.

(1) *Linear static procedure* (LSP). Similar to the elastic analysis procedure in code provisions, LSP uses response spectrum accelerations at the fundamental period as seismic inputs and applies an equivalent lateral force vector to the intended building structure; design parameters such as deflections and member forces are then determined. Unlike the design code provisions, LSP tries to predict 'real' structural responses by using more refined formulas, rather than that in the design code provisions where more conservative response estimates are usually desired.

(2) *Linear dynamic procedure* (LDP). In this procedure, elastic response spectrum analyses are performed followed by a modal superposition technique using SRSS or CQC rules.

(3) *Nonlinear static procedure* (NSP). With this simplified nonlinear analysis procedure commonly known as the static pushover analysis, forces and deformations induced by monotonically increasing lateral loading are evaluated at a target displacement level. More of this procedure will be discussed in Section 3.3.2.

(4) *Nonlinear dynamic procedure* (NDP). This is the most accurate analysis procedure provided that the structural elements and system as well as seismic inputs can be modeled realistically. The response of a building to a set of selected ground motions is determined through numerical integration of the system equations of motion. Inelastic seismic demands can be best predicted.

### 3.3.2 Static pushover analysis

Use of nonlinear time history analysis is impractical in the present design optimization due to its prohibitive computational expenses. The nonlinear static procedure or the pushover analysis will be used instead. It is one of the most popular approximate methods to evaluate seismic structural demands due to its conceptual simplicity (ATC-40 1996; FEMA-273 1997). With this procedure, the nonlinear analytical model of a structural system is statically subjected to monotonically increasing lateral loads, with either a predetermined or an adaptive pattern, that approximate the earthquake-induced inertial force distribution on the structure, until a target displacement level of a controlling point is reached. Seismic strength and deformation demands at this target displacement level are then checked against relevant performance criteria for evaluation purposes.

*Lateral force distributions*

FEMA-273 suggests three lateral force patterns $s^*$ for practical use:

(1) a uniform distribution, with $s_j^* = m_j$ where $j$ = floor number, $m_j$ = mass at the $j$-th floor;

(2) an equivalent lateral force distribution, with $s_j^* = m_j h_j^k$ where $h_j$ = height of the $j$-th floor from the base, $k$ = an exponent factor ($k$ =1 for the fundamental period $T \le 0.5$ sec., $k$ = 2 for $T \ge 2.5$ sec, and linear interpolation for other $T$ values is permitted.);

(3) a square-root-of-sum-of-squares distribution, with $s_j^*$ being defined by the lateral forces back-calculated from the story shears determined by linear elastic response spectrum analysis.

The second lateral force distribution pattern, which is also provided in the 2000 NEHRP provisions (Section 2.1.2), will be used in this study; DRAIN-2DX is used to perform the static pushover analysis with a displacement control option.

*Basic theory*

The following material is based on Krawinkler and Seneviratna (1998). The static pushover analysis uses an 'equivalent' single-degree-of-freedom (SDOF) system analogy to represent the original multi-degree-of-freedom (MDOF) structural system. Assuming that the MDOF system vibrates with a constant shape pattern $\boldsymbol{\varphi}$ that is normalized at a controlling node (e.g., the roof node), the displacement vector of this MDOF system is then $\mathbf{X}(t) = \boldsymbol{\varphi} x_{roof}(t)$. The discretized equations of motion of the MDOF system are

$$\mathbf{M}\boldsymbol{\varphi}\ddot{x}_{roof}(t) + \mathbf{C}\boldsymbol{\varphi}\dot{x}_{roof}(t) + \mathbf{Q}(t) = -\mathbf{M}\mathbf{1}\ddot{x}_g(t) \tag{3.1}$$

where $\mathbf{M}$ = mass matrix, $\mathbf{C}$ = damping matrix, $\mathbf{Q}$ = external force vector, $\ddot{x}_g$ = ground motion acceleration. Pre-multiplying Equation 3.1 by $\boldsymbol{\varphi}^T$ and defining the SDOF displacement as

$$x^*(t) = \left( \frac{\boldsymbol{\varphi}^T \mathbf{M} \boldsymbol{\varphi}}{\boldsymbol{\varphi}^T \mathbf{M} \mathbf{1}} \right) x_{roof}(t) \tag{3.2}$$

leads to

$$M^* \ddot{x}^*(t) + C^* \dot{x}^*(t) + Q^*(t) = -M^* \ddot{x}_g(t) \tag{3.3}$$

where $M^* = \boldsymbol{\varphi}^T \mathbf{M} \mathbf{1}$, $C^* = \left( \frac{\boldsymbol{\varphi}^T \mathbf{M} \mathbf{1}}{\boldsymbol{\varphi}^T \mathbf{M} \boldsymbol{\varphi}} \right) \boldsymbol{\varphi}^T \mathbf{C} \boldsymbol{\varphi}$, $Q^* = \boldsymbol{\varphi}^T \mathbf{Q}$ are the mass, damping, and restoring force, respectively, of the equivalent SDOF system.

Subjected to monotonically increased lateral forces of a usually predefined pattern, the load-deformation characteristics, or the pushover curve, of the MDOF system is typically represented by a base shear vs. roof displacement diagram (Figure 3.3). A bilinear representation is then obtained that defines, for the MDOF system, nominal yield strength $V_y$, yield displacement $\Delta_y$, effective elastic stiffness $K_e$, and straining-hardening stiffness $K_s = \alpha K_e$. The yield strength and yield displacement of the SDOF system are then

$$Q_y^* = \boldsymbol{\varphi}^T \mathbf{Q}_y \tag{3.4}$$

$$\Delta_y^* = \left( \frac{\boldsymbol{\varphi}^T \mathbf{M} \boldsymbol{\varphi}}{\boldsymbol{\varphi}^T \mathbf{M} \mathbf{1}} \right) \Delta_y \tag{3.5}$$

The elastic period of the SDOF system is

$$T^* = 2\pi \sqrt{\frac{\Delta_y^* M^*}{Q_y^*}} \tag{3.6}$$

The strength reduction factor for this SDOF system can be obtained by

$$R = \frac{S_a(T^*) M^*}{Q_y^*} \tag{3.7}$$

where $S_a(T^*)$ is the spectral acceleration at the period $T^*$ of the SDOF system.

The inelastic peak displacement at the controlling node of the MDOF system, $\Delta_u$, is obtained by

$$\Delta_u = \left( \frac{\boldsymbol{\varphi}^T \mathbf{M} \mathbf{1}}{\boldsymbol{\varphi}^T \mathbf{M} \boldsymbol{\varphi}} \right) \Delta_u^* \tag{3.8}$$

where the peak displacement of the SDOF system, $\Delta_u^*$, may be quantified through empirical $R-\mu-T$ relationships, where $\mu = \Delta_u^* / \Delta_y^*$ is the displacement ductility of the SDOF system.

Over the years various $R-\mu-T$ relationships have been proposed (Miranda and Bertero 1994). The one proposed by Nassar and Krawinkler (1991) takes the following form:

$$R = \left[c(\mu - 1) + 1\right]^{1/c} \tag{3.9}$$

where

$$c = \frac{T^a}{1+T^a} + \frac{b}{T} \tag{3.10}$$

with *a* and *b* being strain hardening ratio $\alpha$ -dependent coefficients as given in Table 3.1.

*Application issues*

In general, the static pushover analysis works fairly well for structures that respond primarily in the fundamental mode (usually the first mode). For taller and more flexible structures possibly with mass and/or stiffness irregularity, contributions from higher modes can be significant, for which the pushover analysis may fail to give good estimates of seismic responses. Moreover, behavioral characteristics of structural elements under cyclic loading conditions, such as cumulative damage, are not considered in the pushover analysis. In addition, most of static pushover analysis procedures use time-invariant lateral load patterns, which are a very crude approximation of time-varying height-wise inertial force distribution; static pushover analysis with time-varying adaptive lateral load patterns has been investigated in the literature (e.g., Gupta and Kunnath 2000).

## 3.4 Seismicity for the present study

The target 5%-damped smooth elastic response spectra (Table 3.2, Figure 3.4), which were used to generate sets of SAC ground motion records for the Los Angeles area with soil profile D (Somerville et al. 1997) at two hazard levels corresponding to 50-year exceedance probabilities of 50% and 2% (denoted as 50/50 and 2/50), respectively, are adopted in conjunction with the static pushover analysis to evaluate seismic performance for design optimization problems that will be investigated in the later chapters. Figure 3.5 plots the 50-year and annual exceedance probability vs. spectral acceleration curves for Los Angeles area, assuming a lognormal distribution. Note that these two sets of exceedance probability are related through

$$PE_{annual} = 1 - \left(1 - PE_{50}\right)^{1/50} \tag{3.11}$$

Because of the approximate nature of the static pushover analysis, seismic performance of a code-compliant structural design needs to be further evaluated by the more accurate time history analysis so that possible structural weakness that cannot be captured by the simplified analysis procedure may be exposed and assessed. Sets of twenty SAC ground motion records at 50/50 and 2/50 hazard levels, respectively, whose 5%-damped median elastic response spectra match the above-mentioned target response spectra at 0.3, 1.0, 2.0, and 4.0 sec in a least-square sense, will be used in later chapters to perform the time history analysis in DRAIN-2DX. Tables 3.3 and 3.4 provide the characteristic information of these individual ground motion records at 50/50 and 2/50 hazard levels, respectively, with individual response spectra being plotted in Figure 3.4. Viscous damping ratios are set, at the first mode and at the 0.2 second, to be 4.0%, which is linearly interpolated from 4.3% and 3.6% for typical three- and nine-story steel SMRF buildings, respectively (Lee and Foutch 2000).

**Table 3.1 Coefficients for $R-\mu-T$ relationship (Nassar and Krawinkler 1991)**

| $\alpha$ | $a$ | $b$ |
|---|---|---|
| 0.00 | 1.00 | 0.42 |
| 0.02 | 1.00 | 0.37 |
| 0.10 | 0.80 | 0.29 |

**Table 3.2 Target response spectra values (Somerville et al. 1997)**

| Hazard level | 0.3 sec | 1.0 sec | 2.0 sec | 4.0 sec |
|---|---|---|---|---|
| 50/50 | 0.514 g | 0.288 g | 0.149 g | 0.069 g |
| 2/50 | 1.610 g | 1.190 g | 0.540 g | 0.190 g |

**Table 3.3 Characteristics of SAC 50/50 set of Los Angeles ground motion records**

| ID | Information | Duration [sec] | Magnitude [Mw] | R [km] | Scale | PGA [in/sec/sec] |
|---|---|---|---|---|---|---|
| LA41 | Coyote Lake, 1979 | 39.38 | 5.7 | 8.8 | 2.28 | 227.7 |
| LA42 | Coyote Lake, 1979 | 39.38 | 5.7 | 8.8 | 2.28 | 128.7 |
| LA43 | Imperial Valley, 1979 | 39.08 | 6.5 | 1.2 | 0.40 | 55.4 |
| LA44 | Imperial Valley, 1979 | 39.08 | 6.5 | 1.2 | 0.40 | 43.1 |
| LA45 | Kern, 1952 | 78.60 | 7.7 | 107.0 | 2.92 | 55.7 |
| LA46 | Kern, 1952 | 78.60 | 7.7 | 107.0 | 2.92 | 61.4 |
| LA47 | Landers, 1992 | 79.98 | 7.3 | 64.0 | 2.63 | 130.4 |
| LA48 | Landers, 1992 | 79.98 | 7.3 | 64.0 | 2.63 | 118.8 |
| LA49 | Morgan Hill, 1984 | 59.98 | 6.2 | 15.0 | 2.35 | 123.0 |
| LA50 | Morgan Hill, 1984 | 59.98 | 6.2 | 15.0 | 2.35 | 211.0 |
| LA51 | Parkfield, 1966, Cholame 5W | 43.92 | 6.1 | 3.7 | 1.81 | 301.4 |
| LA52 | Parkfield, 1966, Cholame 5W | 43.92 | 6.1 | 3.7 | 1.81 | 243.8 |
| LA53 | Parkfield, 1966, Cholame 5W | 26.14 | 6.1 | 8.0 | 2.92 | 267.7 |
| LA54 | Parkfield, 1966, Cholame 5W | 26.14 | 6.1 | 8.0 | 2.92 | 305.1 |
| LA55 | North Palm Springs, 1986 | 59.98 | 6.0 | 9.6 | 2.75 | 199.8 |
| LA56 | North Palm Springs, 1986 | 59.98 | 6.0 | 9.6 | 2.75 | 146.3 |
| LA57 | San Fernando, 1971 | 79.46 | 6.5 | 1.0 | 1.30 | 97.7 |
| LA58 | San Fernando, 1971 | 79.46 | 6.5 | 1.0 | 1.30 | 89.2 |
| LA59 | Whittier, 1987 | 39.98 | 6.0 | 17.0 | 3.62 | 296.7 |
| LA60 | Whittier, 1987 | 39.98 | 6.0 | 17.0 | 3.62 | 184.7 |

**Table 3.4 Characteristics of SAC 2/50 set of Los Angeles ground motion records**

| ID | Information | Duration [sec] | Magnitude [Mw] | R [km] | Scale | PGA [in/sec/sec] |
|---|---|---|---|---|---|---|
| LA21 | 1995 Kobe | 59.98 | 6.9 | 3.4 | 1.15 | 495.3 |
| LA22 | 1995 Kobe | 59.98 | 6.9 | 3.4 | 1.15 | 355.4 |
| LA23 | 1989 Loma Prieta | 24.99 | 7.0 | 3.5 | 0.82 | 161.4 |
| LA24 | 1989 Loma Prieta | 24.99 | 7.0 | 3.5 | 0.82 | 182.6 |
| LA25 | 1994 Northridge | 14.95 | 6.7 | 7.5 | 1.29 | 335.3 |
| LA26 | 1994 Northridge | 14.95 | 6.7 | 7.5 | 1.29 | 364.3 |
| LA27 | 1994 Northridge | 59.98 | 6.7 | 6.4 | 1.61 | 357.8 |
| LA28 | 1994 Northridge | 59.98 | 6.7 | 6.4 | 1.61 | 513.4 |
| LA29 | 1974 Tabas | 49.98 | 7.4 | 1.2 | 1.08 | 312.4 |
| LA30 | 1974 Tabas | 49.98 | 7.4 | 1.2 | 1.08 | 382.9 |
| LA31 | Elysian Park (simulated) | 29.99 | 7.1 | 17.5 | 1.43 | 500.5 |
| LA32 | Elysian Park (simulated) | 29.99 | 7.1 | 17.5 | 1.43 | 458.1 |
| LA33 | Elysian Park (simulated) | 29.99 | 7.1 | 10.7 | 0.97 | 302.1 |
| LA34 | Elysian Park (simulated) | 29.99 | 7.1 | 10.7 | 0.97 | 262.8 |
| LA35 | Elysian Park (simulated) | 29.99 | 7.1 | 11.2 | 1.10 | 383.1 |
| LA36 | Elysian Park (simulated) | 29.99 | 7.1 | 11.2 | 1.10 | 424.9 |
| LA37 | Palos Verdes (simulated) | 59.98 | 7.1 | 1.5 | 0.90 | 274.7 |
| LA38 | Palos Verdes (simulated) | 59.98 | 7.1 | 1.5 | 0.90 | 299.7 |
| LA39 | Palos Verdes (simulated) | 59.98 | 7.1 | 1.5 | 0.88 | 193.1 |
| LA40 | Palos Verdes (simulated) | 59.98 | 7.1 | 1.5 | 0.88 | 241.4 |

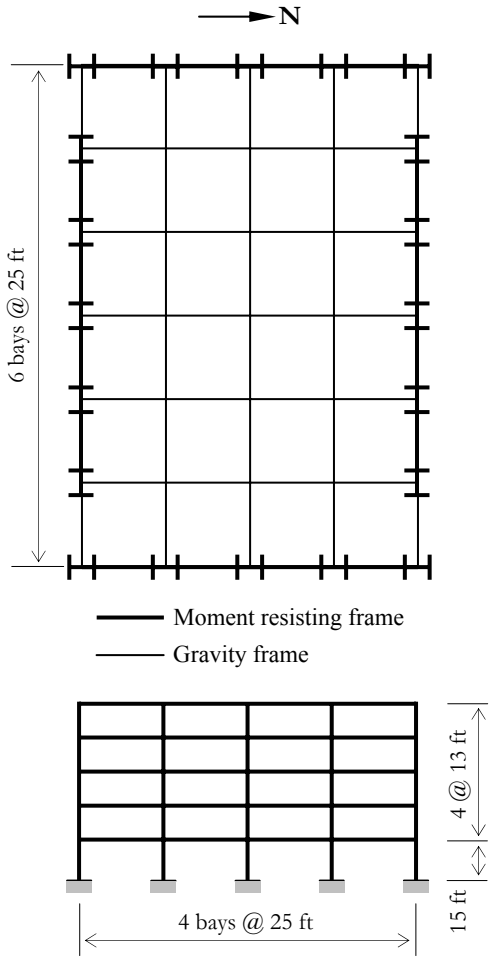


**Figure 3.1 Plan view and elevation of an example steel building**

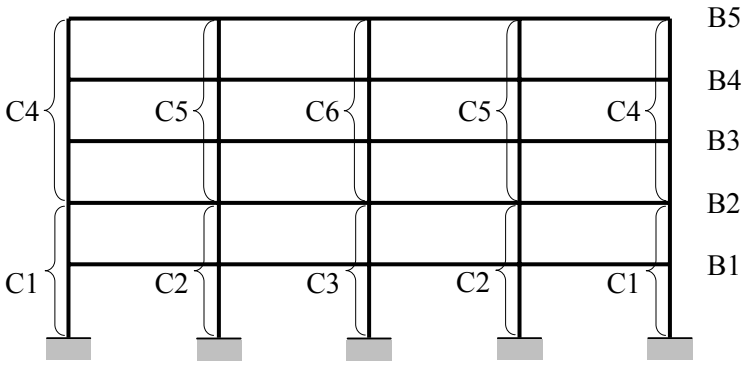


**Figure 3.2 Member linking patterns assumed in the example steel frame**

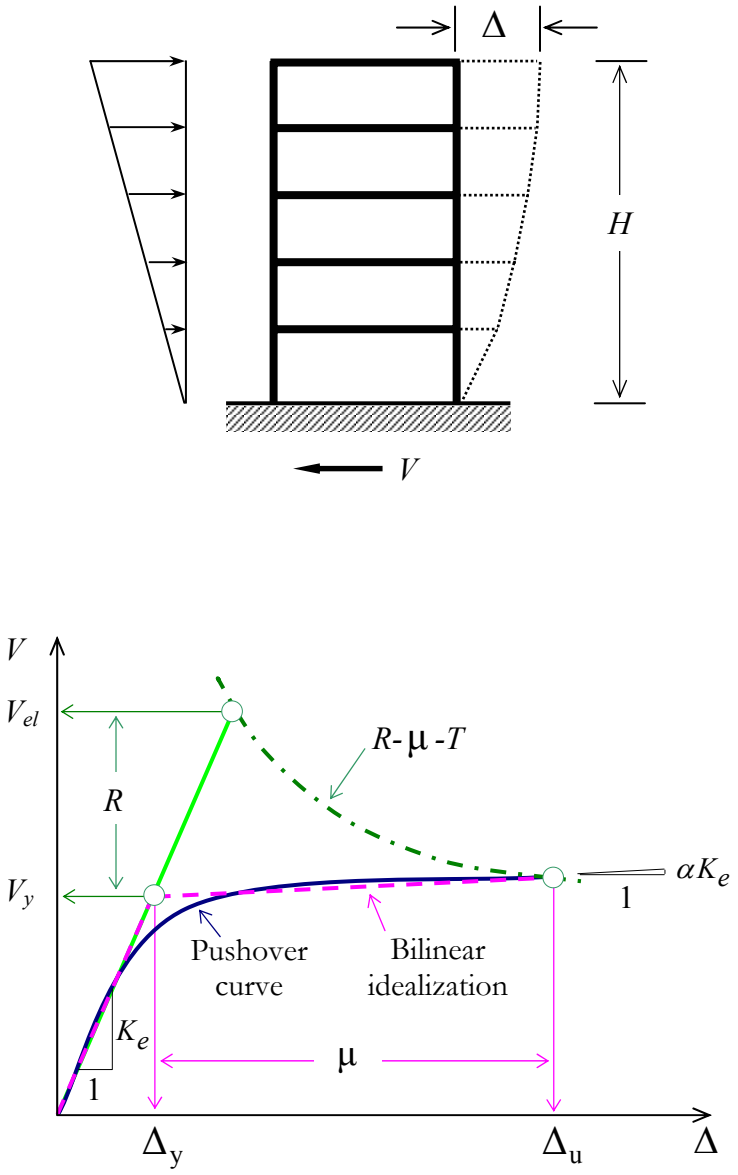


**Figure 3.3 Illustrative sketch of the static pushover analysis**

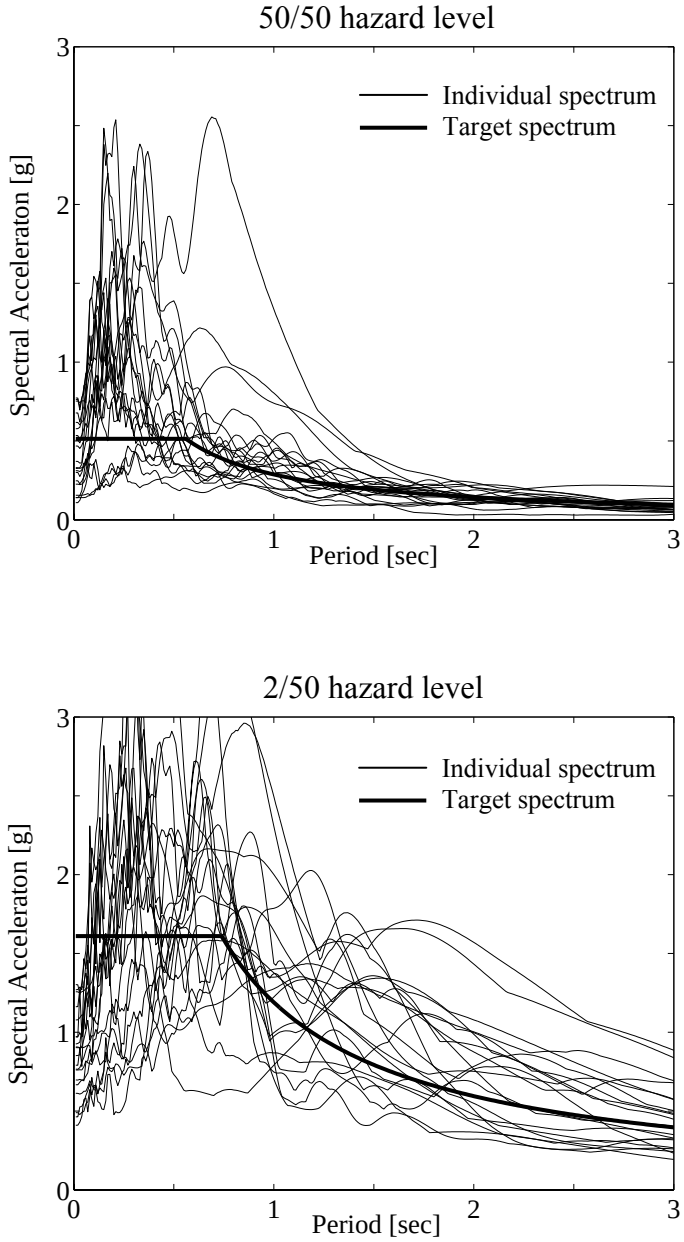


**Figure 3.4 Acceleration response spectra at two hazard levels**

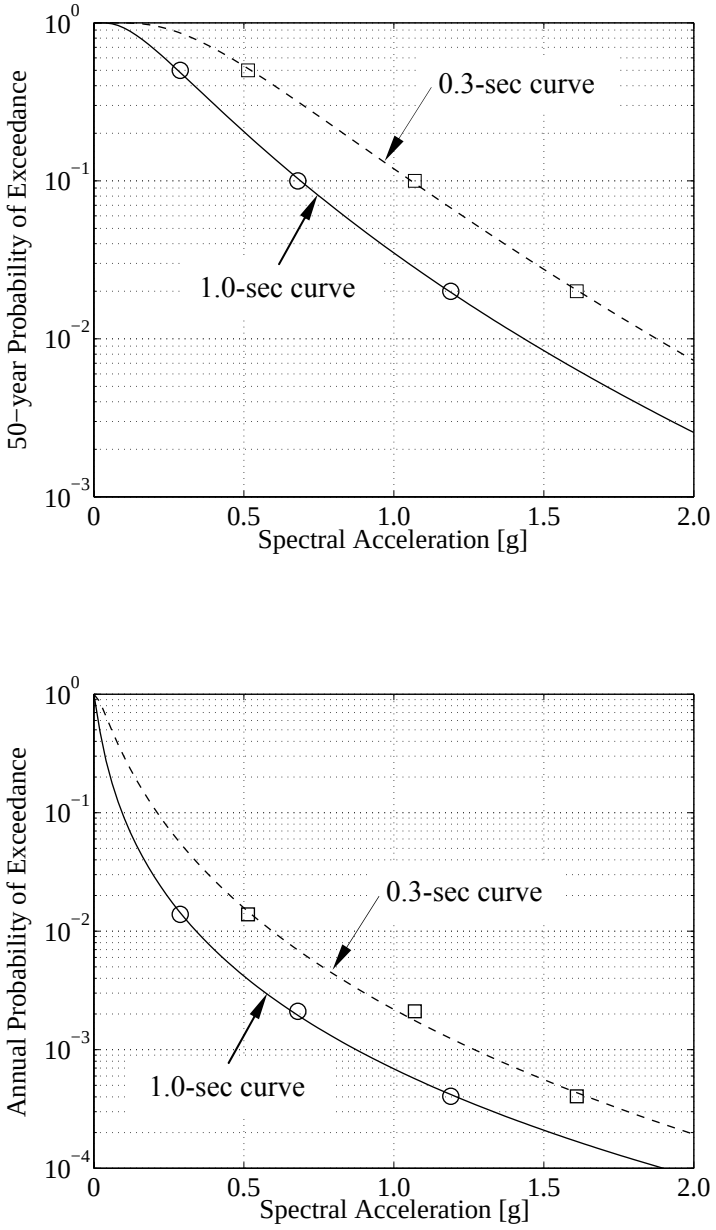


**Figure 3.5 50-year and annual probabilities of exceedance for SAC spectral accelerations**